


## ORIGINAL ARTICLE

# Long noncoding RNA actin filament-associated protein 1 antisense RNA 1 promotes malignant phenotype through binding with lysine-specific demethylase 1 and repressing HMG box-containing protein 1 in non-small-cell lung cancer

Shanxun Yu<sup>1</sup> | Daolu Yang<sup>1</sup> | Yunyao Ye<sup>1,2</sup> | Pei Liu<sup>1,3</sup> | Zhenyao Chen<sup>1</sup> |  
Tianyao Lei<sup>1</sup> | Jiaze Pu<sup>3</sup> | Longfa Liu<sup>3</sup> | Zhaoxia Wang<sup>1,4</sup> 

<sup>1</sup>Department of Oncology, The Second Affiliated Hospital of Nanjing Medical University, Nanjing, China

<sup>2</sup>Department of Oncology, Taizhou People's Hospital, Taizhou, China

<sup>3</sup>Department of Digestive Oncology, The Fourth Affiliated Hospital of Nanjing Medical University, Nanjing, China

<sup>4</sup>Cancer Medical Center, The Second Affiliated Hospital of Nanjing Medical University, Nanjing, China

## Correspondence

Zhaoxia Wang, Department of Oncology, The Second Affiliated Hospital of Nanjing Medical University, Nanjing, China.  
Email: zhaoxiawang66@126.com.

## Funding information

National Natural Science Foundation of China, Grant/Award Number: 81672307 and 81871871; the Medical Innovation Team Foundation of the Jiangsu Provincial Enhancement Health Project, Grant/Award Number: CXTDA2017021; the "333 high class Talented Man Project", Grant/Award Number: BRA2016509; the Nanjing Science and Technology Development Project, Grant/Award Number: 2017sc512046; the Jiangsu Graduate Scientific Research Innovation Program, Grant/Award Number: KYCX18\_1494

## Abstract

The number of documented long noncoding RNAs (lncRNAs) has dramatically increased, and their biological functions and underlying mechanisms in pathological processes, especially cancer, remain to be elucidated. Actin filament-associated protein 1 antisense RNA 1 (AFAP1-AS1) is a 6810-nt lncRNA located on chromosome 4p16.1 that was first reported to be upregulated in esophageal adenocarcinoma tissues and cell lines. Here we reported that AFAP1-AS1, recruiting and binding to lysine-specific demethylase 1 (LSD1), was generally overexpressed in human non-small-cell lung cancer (NSCLC) tissues using quantitative real-time PCR. Higher AFAP1-AS1 expression was significantly correlated with larger tumor size ( $P = .008$ ), lymph node metastasis ( $P = .025$ ), higher TNM stage ( $P = .024$ ), and worse overall survival in NSCLC patients. In vitro experiments revealed that AFAP1-AS1 downregulation inhibited cell migration and induced apoptosis; AFAP1-AS1 knockdown also hindered tumorigenesis in vivo. Moreover, mechanistic investigations including RNA immunoprecipitation and ChIP assays validated that AFAP1-AS1 repressed HMG box-containing protein 1 (HBP1) expression by recruiting LSD1 to the HBP1 promoter regions in PC-9 and H1975 cells. Furthermore, HBP1 functions as a tumor suppressor, and its ectopic expression hindered cell proliferation. Rescue assays determined that the oncogenic effect of AFAP1-AS1 is partially dependent on the epigenetic silencing of HBP1. In conclusion, our results indicate that AFAP1-AS1 is carcinogenic and that the AFAP1-AS1/LSD1/HBP1 axis could constitute a new therapeutic direction for NSCLC.

## KEYWORDS

AFAP1-AS1, HBP1, long noncoding RNA, LSD1, non-small-cell lung cancer

Shanxun Yu, Daolu Yang, and Yunyao Ye equally contributed to this work.

This is an open access article under the terms of the Creative Commons Attribution-NonCommercial License, which permits use, distribution and reproduction in any medium, provided the original work is properly cited and is not used for commercial purposes.

© 2019 The Authors. *Cancer Science* published by John Wiley & Sons Australia, Ltd on behalf of Japanese Cancer Association.

## 1 | INTRODUCTION

Lung cancer is the most commonly diagnosed cancer and the leading cause of cancer-related deaths in men worldwide.<sup>1</sup> Non-small-cell lung cancer (NSCLC), a more prevalent lung cancer subtype, accounts for approximately 80%-85% of all cases.<sup>2</sup> Although the treatment of surgical operation, chemotherapy, radiotherapy, targeted therapy, and immunotherapy is widely carried out, only 15% of NSCLC patients survive more than 5 years.<sup>3</sup> One of most important reasons behind the high incidence and low 5-year survival rate of NSCLC is the low rate of early detection/diagnosis. Therefore, the limitations of current diagnostic and treatment approaches should be considered in future work aimed at developing a more complete investigation of the underlying cellular activities or molecular mechanisms in NSCLC tumorigenesis, as these studies could provide novel biomarkers and therapeutic targets.

Advances in next-generation deep sequencing and bioinformatics technologies confirm that only 1%-2% of the human genome can encode proteins.<sup>4</sup> Based on their length, RNAs without coding potential are divided into two subclasses: (a) small or short non-coding RNAs; and (b) long noncoding RNAs (lncRNAs;  $\geq 200$  nt). Recent research has revealed that lncRNAs have dramatic impacts on multiple biological processes through diverse mechanisms, including translational inhibition, mRNA degradation, RNA decoys, recruiting chromatin modifiers, and regulating protein activity.<sup>5</sup> Interestingly, emerging evidence has revealed that aberrant lncRNA expression is involved in human diseases, especially cancers.<sup>6-8</sup> For instance, lncRNA TINCR promotes the proliferation of gastric cancer cells by binding to Staufin1 protein and subsequently influencing KLF2 expression and mRNA stability.<sup>9</sup> Furthermore, our previous studies showed that lncRNA MEG3 is significantly downregulated in lung adenocarcinoma, and partially reverses cisplatin resistance in LAD cells through p53/Bcl-xl-induced mitochondrial-directed apoptosis.<sup>10</sup> Additionally, LINC01234 can exert oncogenic function by serving as a competing endogenous RNA for microRNA (miR)-204-5p that regulates core-binding factor  $\beta$  expression in gastric cancer.<sup>11</sup>

Actin filament-associated protein 1 antisense RNA 1 (AFAP1-AS1) is an lncRNA transcribed from the antisense DNA strand of the AFAP1 gene and was first reported to be upregulated in esophageal adenocarcinoma tissues and cell lines.<sup>12</sup> Further work showed that AFAP1-AS1 was upregulated in lung adenocarcinoma, gastric cancer, pancreatic ductal adenocarcinoma, cholangiocarcinoma, colorectal cancer, and nasopharyngeal carcinoma, where it was associated with progression and poor prognoses.<sup>13-19</sup> Previous studies also suggested that AFAP1-AS1 participated in cell proliferation, apoptosis, and invasion by regulating PTEN/p-AKT and RhoA/Rac2 signaling.<sup>20,21</sup> Nevertheless, elucidating the oncogenic functions of AFAP1-AS1 in NSCLC development and progression requires further effort. Here, we investigated the effect of AFAP1-AS1 on NSCLC cell proliferation and migration *in vitro* and *in vivo* and identified novel targets and mechanisms of AFAP1-AS1, which could fully elucidate its critical role in the pathological processes of NSCLC.

## 2 | MATERIALS AND METHODS

### 2.1 | Differential expression analysis

Lung cancer gene expression data were downloaded from The Cancer Genome Atlas (TCGA) and Gene Expression Omnibus (GEO) dataset. The independent datasets from GSE31210, GSE19804, GSE18842, and GSE19188 were analyzed in this study. The BAM files and normalized probe-level intensity files were downloaded from TCGA and GEO databases, respectively. The probe sequences were downloaded from GEO or microarray manufacturers, and Bowtie was used to re-annotate probes according to GENCODE Release 20 annotation for lncRNAs. For multiple probes corresponding to one gene, the probe with the maximum signal was selected to generate expression of lncRNAs. The Kaplan-Meier curve was used to test lncRNA association with time to progression. For verifying expression correlation between genes, Pearson's correlation analysis was used after CEL files from GSE19804 were downloaded and normalized by Robust Multichip Average.

### 2.2 | Tissue sample collection

We acquired 96 pairs of lung cancer and adjacent normal tissues from patients who underwent surgery at The Second Affiliated Hospital of Nanjing Medical University (Nanjing, China) between 2010 and 2013. Patients were diagnosed with NSCLC based on imaging examination and histopathological analysis, no preoperative adjuvant chemotherapy was undertaken before surgical operation. All collected tissues were snap frozen in liquid nitrogen and stored at  $-80^{\circ}\text{C}$  until required. Table 1 summarizes the clinicopathological characteristics, including tumor size, lymph node metastasis, and advanced TNM staging. We obtained written informed consent from all patients before surgery and the study was approved by the Research Ethics Committee of The Second Affiliated Hospital of Nanjing Medical University (IRB number: 09036304).

### 2.3 | Cell culture

The normal human bronchial epithelial cell line (16HBE) and another five NSCLC cell lines (A549, SPC-A1, PC-9, H1299, and H1975) were maintained in RPMI-1640/DMEM (Gibco, Grand Island, NY, USA) supplemented with 10% newborn calf serum (NBGS; PAA Laboratories, Haidmannweg, Australia) and 1% penicillin (100 U/mL)/streptomycin (100  $\mu\text{g/mL}$ ; Invitrogen, Carlsbad, CA, USA) in a 5%  $\text{CO}_2$  and humidified atmosphere at  $37^{\circ}\text{C}$ .

### 2.4 | RNA extraction and quantitative PCR assays

Total RNA was isolated from tissues or cultured cells using TRIzol reagent (Invitrogen Life Technologies). After removal of genomic DNA using gDNA Eraser for 2 minutes at  $4^{\circ}\text{C}$ , 1  $\mu\text{g}$  total RNA was reverse transcribed to a final volume of 20  $\mu\text{L}$  master mix with the PrimeScript RT Reagent Kit with gDNA Eraser (TaKaRa, Dalian, China). Using the synthesized cDNA

**TABLE 1** Correlation between actin filament-associated protein 1 antisense RNA 1 (AFAP1-AS1) expression and clinicopathological characteristics of patients with non-small-cell lung cancer (n = 96)

Characteristics	AFAP1-AS1 low, n (%)	AFAP1-AS1 high, n (%)	P value, $\chi^2$ test
Age (years)			
≥55	23 (47.9)	26 (54.2)	0.540
<55	25 (52.1)	22 (45.8)	
Gender			
Male	27 (56.2)	26 (54.2)	0.837
Female	21 (43.8)	22 (45.8)	
Histological subtype			
Adenocarcinoma	24 (50)	28 (58.3)	0.413
Squamous cell carcinoma	24 (50)	20 (41.7)	
TNM stage			
I-II	32 (66.7)	21 (43.8)	0.024 <sup>*</sup>
III-IV	16 (33.3)	27 (56.2)	
Tumor size			
≥5 cm	17 (35.4)	30 (62.5)	0.008 <sup>**</sup>
<5 cm	31 (64.6)	18 (37.5)	
Lymph node metastasis			
Negative	30 (62.5)	19 (39.6)	0.025 <sup>*</sup>
Positive	18 (27.5)	29 (60.4)	
Smoking history			
Smokers	28 (58.3)	23 (47.9)	0.306
Never smokers	20 (41.7)	25 (52.1)	

\* $P < .05$ ; \*\* $P < .01$ .

as a template, we prepared 20  $\mu$ L cDNA mixture by SYBR Premix Ex Taq (TaKaRa). The quantitative real-time (qRT)-PCRs were carried out on a Mastercycler Ep Realplex system (Eppendorf, Hamburg, Germany) to detect the consistent amplification. Specific primer sequences are listed in Table S1. Our qRT-PCR results were based on relative threshold cycle (CT) values, and then in the form of fold changes ( $2^{-\Delta\Delta CT}$ ).

## 2.5 | RNA interference

Small interfering RNAs were transfected into PC-9 and H1975 cells using Lipofectamine 2000 (Invitrogen). We purchased three individual AFAP1-AS1 siRNAs (si-AFAP1-AS1 1#, 2#, and 3#), scrambled negative control siRNA (si-scrambled), enhancer of zeste homolog 2 (EZH2) siRNA, and lysine-specific demethylase 1 (LSD1) siRNA from GenePharma (Shanghai, China). These siRNA sequences are summarized in Table S1. Cells were collected for experiment analysis after 48 hours of incubation.

## 2.6 | Plasmid generation

The pCDNA-HMG box-containing protein 1 (HBP1) vector was synthesized by subcloning the HBP1 sequence (NM\_001244262) into

the pCDNA3.1 vector (YouBio, Hunan, China), and pCDNA3.1 vector was used as a control group. Plasmid vectors were transfected into NSCLC cells by X-tremeGENE HP DNA transfection reagent (Roche, Basel, Switzerland).

## 2.7 | Cell proliferation assays

The CCK-8 method (Promega, Madison, WI, USA) was used to detect the living cells over time according to the manufacturer's instructions. Transfected PC-9 and H1975 cells, 1250 cells and 200  $\mu$ L culture medium for each well, were grown in 96-well plates with five replicate wells and the relative cell growth was detected every 24 hours. The absorbance was measured at 450 nm after adding 20  $\mu$ L CCK-8 solution to each well for 2 hours. In the colony formation assay, transfected cells (n = 500) were placed in a 6-well plate supplemented with 2 mL DMEM or RPMI-1640 containing 10% NBS each well for 14 days. The cloned spots formed by the cells were fixed with methanol, then stained with 0.1% crystal violet (Meryer, Shanghai, China) and counted manually.

## 2.8 | Apoptosis and cell cycle analysis by flow cytometry

PC-9 and H1975 cells transfected with AFAP1-AS1-siRNAs or HBP1-expressing plasmid were collected after 48 hours by trypsinization. Cells were resuspended in 1 $\times$  binding buffer containing FITC-annexin V and propidium iodide (PI) for double staining according to the manufacturer's instructions. Flow cytometry (FACScan; BD Biosciences, Franklin Lakes, NJ, USA) was used to analyze cells with CellQuest software (BD Biosciences). The cells were divided into viable cells, dead/damaged cells, early apoptotic cells and late apoptotic cells, and the percentage of apoptotic cells in each experiment were analyzed and compared by software. In the cell cycle analysis, cells were subjected to PI staining using CycleTEST + DNA Reagent Kit (BD Biosciences) and analyzed by FACScan flow cytometry, cells of G<sub>0</sub>/G<sub>1</sub>, S, and G<sub>2</sub>/M phase were counted and compared.

## 2.9 | Western blot analysis and Abs

Cell protein lysates were separated by SDS-PAGE (Bio-Rad, Hercules, CA, USA) and transferred to 0.45  $\mu$ m PVDF transfer membranes (Thermo Fisher Scientific, Rockford, IL, USA). The membrane was blocked with 5% nonfat dry milk in 0.1% TBS-Tween-20 (TBST) for 2 hours, and then incubated with primary Abs for the night. The blots were washed with TBST three times for approximately 5 minutes a time, followed by incubation with HRP-conjugated secondary Abs. Enhanced chemiluminescent HRP substrate was used for quantification by densitometry (Quantity One software; Bio-Rad). Anti-GAPDH (Proteintech Group, Chicago, IL, USA) was used as a control. Anti-HBP1 was purchased from Santa Cruz Biotechnology (Dallas, TX, USA). Anti-LSD1 was purchased from Cell Signaling Technology (Boston, MA, USA).

## 2.10 | Cell migration assays

Using Transwells (8.0- $\mu\text{m}$  pores; Corning, Tewksbury, MA, USA) for migration assays, 300  $\mu\text{L}$  medium containing 1% NBCS and  $2.5 \times 10^4$  NSCLC cells was transferred to the upper chamber. Medium containing 10% NBCS without cells were transferred to the lower chamber. After incubation at 37°C for 48 hours, we used cotton wool to wipe off the cells remaining on the upper membrane. The other cells that migrated to the lower membrane were fixed and stained, followed by photographing with an IX51 inverted microscope (Olympus, Tokyo, Japan).

## 2.11 | 5-Ethynyl-2'-deoxyuridine analysis

The 5-ethynyl-2'-deoxyuridine (EdU) labelling kit (Ribobio) was used to detect cell viability. The 12-well plate incubated  $5 \times 10^4$  cells per well, and cells following 48 hours transfection were incubated with 300  $\mu\text{L}$  diluted EdU labelling media for 2 hours in the cell culture CO<sub>2</sub> incubator. After cell immobilization in 4% paraformaldehyde and 0.5% Triton X-100, cells were reacted with Apollo reaction liquid for 30 minutes in the dark at room temperature. We used DAPI as a nuclear/chromosomal counterstain. The EdU-positive cells were observed and photographed under a fluorescence microscope. Each treatment group was checked by five fields of view randomly.

## 2.12 | Tumor formation assay in vivo

The animal experiment protocols were approved by The Animal Ethical and Welfare Committee of Nanjing Medical University and were in strict accordance with the Guide for the Care and Use of Laboratory Animals of the NIH. We resuspended PC-9 cells, stably transfected with sh-AFAP1-AS1 or empty vector, at a concentration of  $2 \times 10^7$  cells/mL in PBS. The BALB/c nude mice (4 weeks old) were s.c. injected with 100  $\mu\text{L}$  of suspended cells on either side of the armpit regions. The measurement of tumor size was repeated every 3 days, and tumor size was calculated by the formula: volume = length  $\times$  width<sup>2</sup>  $\times$  0.5. At 15 days after injection, mice were killed, and the size and weight of resected tumors was tested. The tumors were also subjected to the qRT-PCR analysis of AFAP1-AS1 expression and immunohistochemical staining analysis of Ki-67.

## 2.13 | Subcellular fractionation

Subcellular fractionation assays were carried out using the PARIS Kit (Life Technologies). According to the manufacturer's instructions, the cells can be separated into nuclear and cytoplasmic fractions before undergoing the RNA isolation procedure.

## 2.14 | RNA immunoprecipitation assays

The identification of RNA species associated with RNA-binding protein was determined with a Magna RIP RNA-Binding Protein Immunoprecipitation Kit (Millipore, Billerica, MA, USA). PC-9 and

H1975 cells at 80%-90% confluency were scraped off from the culture dishes, then dispersed in complete RNA immunoprecipitation (RIP) lysis buffer for RIP lysate preparation. The samples included magnetic beads, negative control Ab IgG, and candidate Ab LSD1, EZH2, or SUZ12 (Millipore) to prepare bead-Ab complexes. Then the supernatants of thawed RIP lysate and treated beads were incubated with RIP immunoprecipitation buffer in tubes rotating overnight at 4°C. Then the immunoprecipitate was incubated with proteinase K buffer in tubes shaking at 55°C for 30 minutes to digest the protein. Finally, the isolated and purified RNA was subjected to the qRT-PCR analysis to elucidate the presence of AFAP1-AS1.

## 2.15 | Chromatin immunoprecipitation assays

Chromatin immunoprecipitation (ChIP) assays were carried out using the Magna ChIP A Kit according to the manufacturer's protocol (Millipore). PC-9 and H1975 cells at 80%-90% confluency in a 15-cm culture dish were prepared for cross-linking and lysis, which were treated with formaldehyde and incubated at room temperature for 10 minutes. After sonication of cell lysates to generate sheared cross-linked chromatin of 200-1000 base pairs in length, the immunoprecipitation of cross-linked chromatin was undertaken by adding 20  $\mu\text{L}$  of suspended protein A magnetic beads and 5.0  $\mu\text{g}$  LSD1 Ab (Millipore), H3 trimethyl Lys 4 Ab (Millipore), or IgG as control per tube. After the elution of protein/DNA complexes, free and purified DNA was detected by qPCR.

## 2.16 | Immunohistochemistry

The primary tumors were subjected to immunohistochemical staining analysis of Ki-67 protein levels as previously described.

## 2.17 | Statistical analysis

All statistical analyses were carried out using SPSS 20.0 software (IBM, Armonk, NY, USA). The significance of differences in experimental data between different groups was estimated by Student's *t* test, and GraphPad Prism 5.0 (GraphPad Software, La Jolla, CA, USA) was used to draw all the plots. The correlations between AFAP1-AS1 expression and the clinical features of NSCLC patients were examined by the  $\chi^2$  test. The Kaplan-Meier method was used to draw progression-free survival and overall survival curves, and the log-rank test was applied for comparison. All tests were two-sided, and *P* values less than .05 were chosen for statistically significant.

# 3 | RESULTS

## 3.1 | Antisense-transcribed lncRNA AFAP1-AS1 upregulated in tissues and cell lines

To identify expression levels of AFAP1-AS1 in NSCLC cancerous tissues compared with noncancerous tissues, four microarray datasets

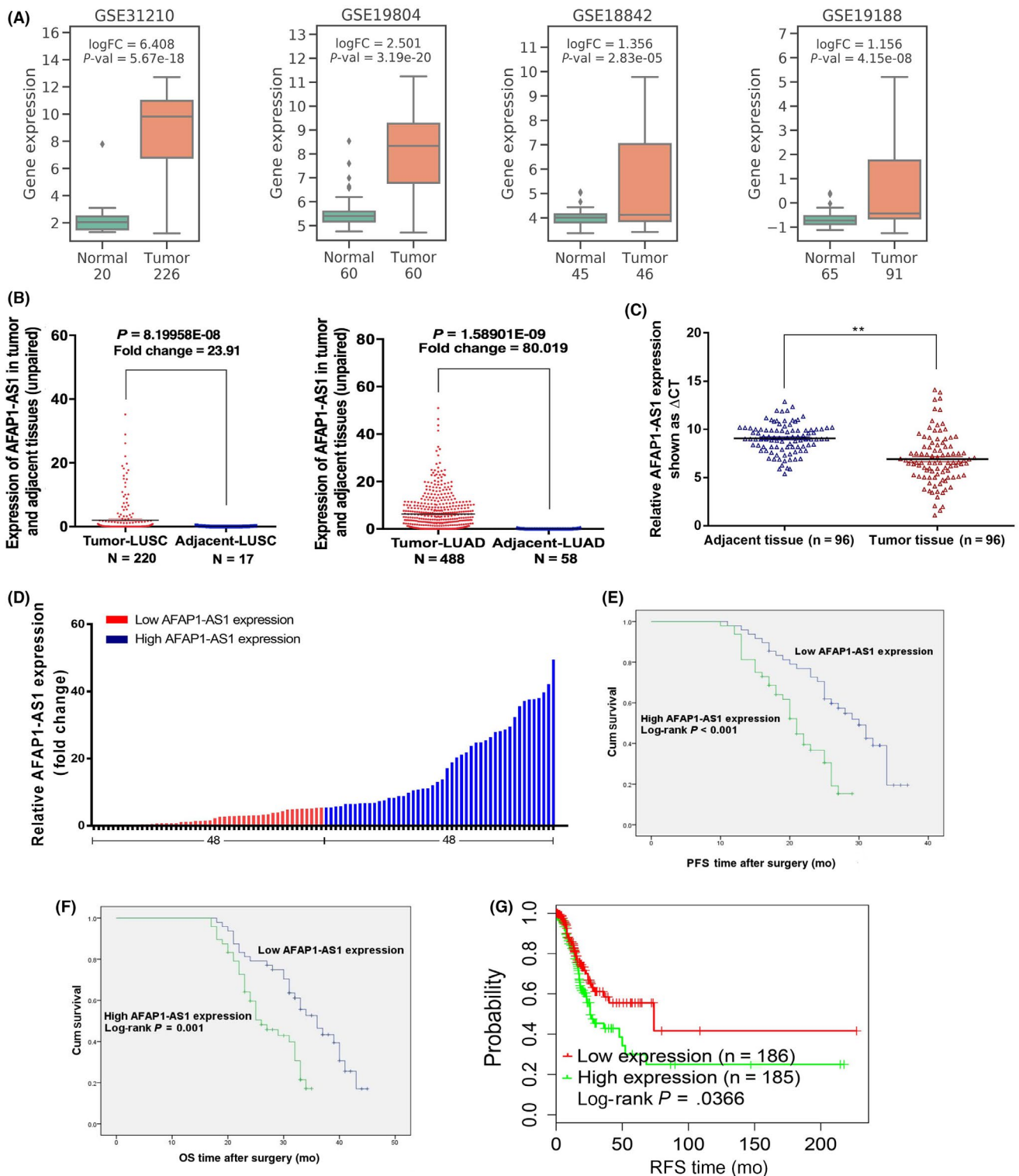


**FIGURE 1** Relative actin filament-associated protein 1 antisense RNA 1 (AFAP1-AS1) expression levels in non-small-cell lung cancer (NSCLC) tissues and its clinical relevance. A, Relative expression of AFAP1-AS1 in NSCLC cancer tissues compared with normal tissues was analyzed by using Gene Expression Omnibus datasets including GSE31210, GSE19804, GSE18842, and GSE19188. B, Relative expression of AFAP1-AS1 in lung squamous cell carcinoma (LUSC) and lung adenocarcinoma (LUAD) tissues compared with normal tissues was analyzed using The Cancer Genome Atlas dataset. C, Relative expression of AFAP1-AS1 in NSCLC tissues compared with adjacent normal tissues (n = 96) was detected by quantitative real-time PCR, and normalized to GAPDH expression. D, The patients (n = 96) were divided into two groups according to AFAP1-AS1 expression. E, F, Kaplan-Meier progression-free survival (PFS) (E) and overall survival (OS) (F) curves according to AFAP1-AS1 expression levels. G, Kaplan-Meier curves of recurrence-free survival (RFS) in LUAD patients, by using data from TCGA-LUAD. Patients were grouped by the median AFAP1-AS1 expression. Data are presented as the mean  $\pm$  SEM. \* $P < .05$ , \*\* $P < .01$

(GSE31210, GSE19804, GSE18842, and GSE19188) were obtained from GEO datasets. As a result, AFAP1-AS1 expression levels were upregulated in NSCLC tumor tissues (Figure 1A), and sequencing data from TCGA also confirmed the high expression of AFAP1-AS1 in human lung squamous cell carcinoma and human lung adenocarcinoma tissues compared with normal tissues (Figure 1B). In addition, we analyzed AFAP1-AS1 expression in 96 paired NSCLC and adjacent normal tissues using qRT-PCR normalized to GAPDH, and relatively high expression was found in 78 of 96 samples (fold change >1.2; Figure 1C).

Moreover, to analyze correlations between AFAP1-AS1 expression and the clinical features of NSCLC patients, the 96 NSCLC patients were classified into two groups according to the median ratio (fold-change = 5.531) of relative AFAP1-AS1 expression in tumor tissues: (a) the high AFAP1-AS1 group (n = 48, AFAP1-AS1 expression ratio  $\geq 5.531$ ), and (b) the low AFAP1-AS1 group (n = 48, AFAP1-AS1 expression ratio  $\leq 5.531$ ) (Figure 1D). As indicated in Table 1, the high AFAP1-AS1 group showed larger tumor size ( $P = .008$ ), lymph node metastasis ( $P = .025$ ), and a higher TNM stage ( $P = .024$ ), but was not correlated with other characters including age ( $P = .54$ ), sex ( $P = .837$ ), histological subtype ( $P = .413$ ), and smoking history ( $P = .306$ ). Kaplan-Meier survival analysis showed that patients with high AFAP1-AS1 expression had shorter overall survival and progression-free survival times than those with low AFAP1-AS1 expression (Figure 1E,F). As shown in Figure 1F, the median overall survival time for the low AFAP1-AS1 expression group was  $36 \pm 2.602$  months, while for the high AFAP1-AS1 expression group it was only  $26 \pm 2.209$  months; progression-free survival times showed the same trend. Furthermore, by generating Kaplan-Meier curves of recurrence-free survival using survival data from TCGA, we found that the lung adenocarcinoma patients with high AFAP1-AS1 expression also had significantly worse recurrence-free survival ( $P < .05$ ) (Figure 1G). Thus, dysregulation of AFAP1-AS1 is a key event involving a poor prognosis of NSCLC.

### 3.2 | In vitro effects of AFAP1-AS1 on proliferation, apoptosis, and cell cycle progression

To investigate the biological functions of AFAP1-AS1 in NSCLC cells, we first determined relative AFAP1-AS1 expression in the normal bronchial epithelial cell line 16HBE and five human NSCLC cell lines (H1975, PC-9, A549, SPC-A1, and H1299) by qRT-PCR. As shown in Figure 2A, PC-9 and H1975 cells had the highest relative AFAP1-AS1 expression compared with 16HBE cells. Next, we synthesized three siRNAs to knock down AFAP1-AS1 expression; si-AFAP1-AS1 1# and 3# had higher interference efficiencies than si-AFAP1-AS1 2# following transfection (Figure 2B). The CCK-8 assays indicated that the viability of PC-9 and H1975 cells with AFAP1-AS1-siRNA 1#/3#

treatment was significantly reduced compared with cells transfected with scrambled siRNA (Figure 2C). Consistently, the colony formation abilities of NSCLC cells were impaired following transfection with si-AFAP1-AS1 (Figure 2D). Similar differences were confirmed in the EdU/DAPI immunostaining analysis (Figure 2E).

In order to determine whether cell cycle distribution and apoptosis were altered following AFAP1-AS1 knockdown in NSCLC cells, we undertook flow cytometric assays. Flow cytometric analysis revealed that PC-9 and H1975 cells transfected with si-AFAP1-AS1 1# or 3# had higher rates of apoptosis and  $G_0/G_1$  cell cycle arrest compared with cells transfected with scrambled siRNA (Figure 3A,B). Taken together, these data indicated that AFAP1-AS1 promoted the proliferation of lung cancer cells by inhibiting apoptosis and promoting cell cycle transition.

### 3.3 | Downregulating AFAP1-AS1 inhibited NSCLC cell migration

Cancer cell invasion and migration play important roles during cancer onset and progression. Using Transwell assays, we found that PC-9 and H1975 cell migration was significantly impeded following AFAP1-AS1 knockdown (Figure 3C).

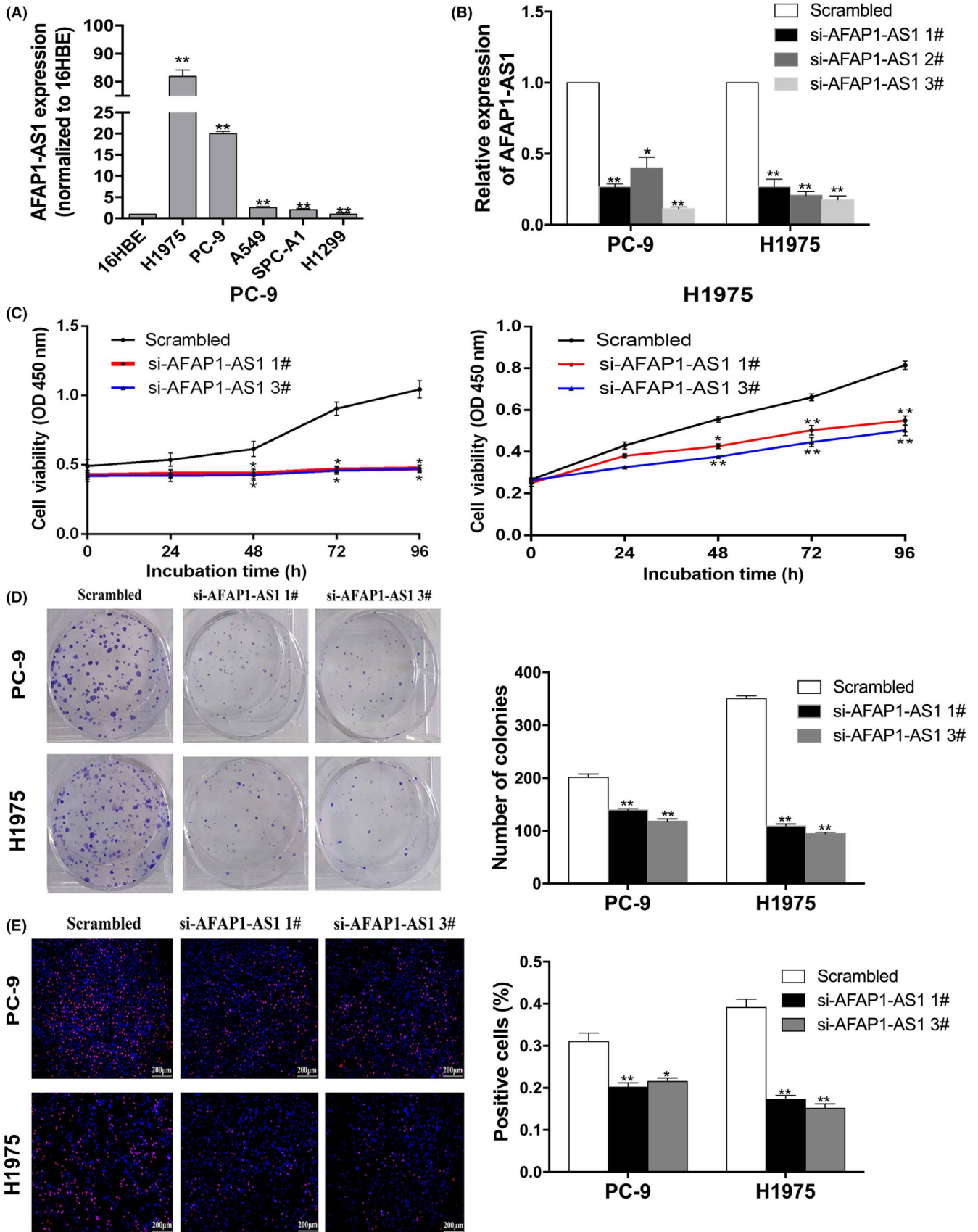
### 3.4 | Xenograft mouse model shows that AFAP1-AS1 knockdown impedes tumor growth

To confirm our in vitro results in an in vivo model, male nude mice were inoculated with PC-9 cells stably expressing sh-AFAP1-AS1 or empty vector. Fifteen days after s.c. injection, the tumors that developed from AFAP1-AS1-silenced PC-9 cells were significantly smaller in size than those formed by cells expressing empty vector (Figure 4A); these data were consistent with tumor growth data (Figure 4B). Moreover, there was a significant decrease of xenograft tumor weight in the sh-AFAP1-AS1 group compared with the control group (Figure 4C). The qRT-PCR analysis confirmed that tumor tissues of the sh-AFAP1-AS1 group showed lower AFAP1-AS1 expression (Figure 4D). Next, immunohistochemical analysis revealed that tumors with stable AFAP1-AS1 knockdown showed decreased Ki-67 positivity than those from the empty vector group (Figure 4E). Our findings indicated that AFAP1-AS1 plays an oncogenic role that promotes a proliferative phenotype in NSCLC cells in vivo.

### 3.5 | Underlying target of AFAP1-AS1 is HBP1

To investigate possible modulation of the sense gene AFAP1 by its antisense transcript AFAP1-AS1, we analyzed changes in

**FIGURE 2** Effects of actin filament-associated protein 1 antisense RNA 1 (AFAP1-AS1) on non-small-cell lung cancer (NSCLC) cell proliferation in vitro. A, Quantitative real-time (qRT)-PCR analysis of AFAP1-AS1 expression in NSCLC cells lines (H1975, PC-9, A549, SPC-A1, and H1299), compared with that in normal human bronchial epithelial cells (16HBE). B, qRT-PCR analysis of AFAP1-AS1 expression in PC-9 and H1975 cells transfected with si-AFAP1-AS1 1#, si-AFAP1-AS1 2#, si-AFAP1-AS1 3#, and scrambled siRNA. C, CCK-8 assays were carried out to determine the cell viability of si-AFAP1-AS1-transfected PC-9 and H1975 cells. D,E, Colony formation assays (D) and EdU staining assays (E) were used to test the proliferation of si-AFAP1-AS1-transfected PC-9 and H1975 cells. Representative images and data are based on three independent experiments. Data are presented as the mean  $\pm$  SEM. \* $P < .05$ , \*\* $P < .01$



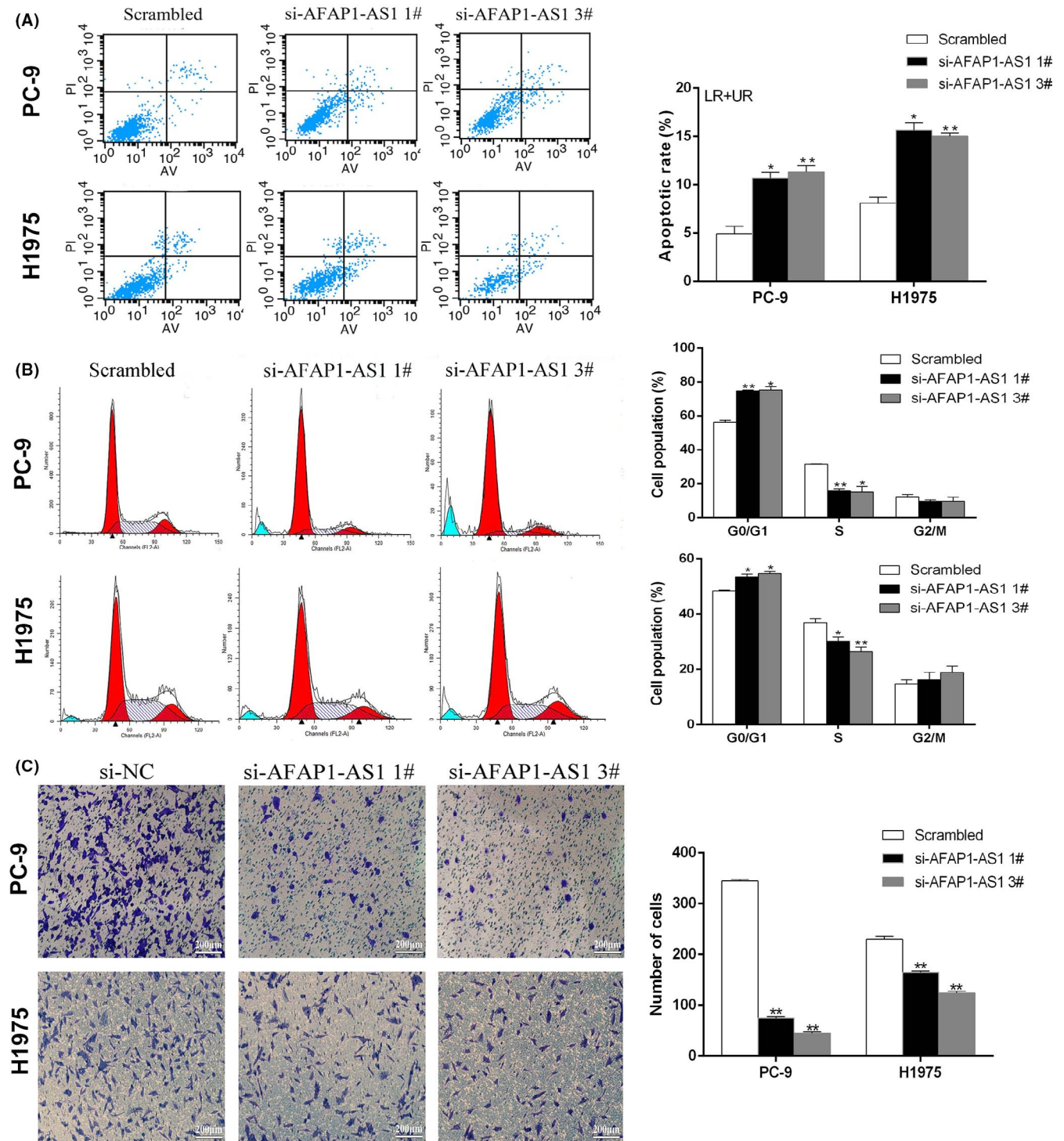


**FIGURE 3** Knockdown of actin filament-associated protein 1 antisense RNA 1 (AFAP1-AS1) induced apoptosis and inhibited cell cycle and migration in vitro. A, 48 h after transfection, non-small-cell lung cancer (NSCLC) cells were stained and analyzed by flow cytometry. LR, early apoptotic cells; UR, terminal apoptotic cells. B, Percentage of cells in G<sub>0</sub>/G<sub>1</sub>, S, or G<sub>2</sub>/M phase was analyzed by flow cytometry when NSCLC cells transfected with si-AFAP1-AS1. C, Transwell assays were used to determine representative migratory abilities of PC-9 and H1975 cells

AFAP1 expression following AFAP1-AS1 silencing, and found that AFAP1 mRNA levels remained unchanged (Figure S1A). To further study the molecular mechanisms underlying AFAP1-AS1 activity in PC-9 and H1975 cells, we first used subcellular fractionation

assays to examine its distribution in cells. The results showed that AFAP1-AS1 RNA was primarily located within nuclear fractions (Figure 5A), indicating that its regulation might occur at the transcriptional level.



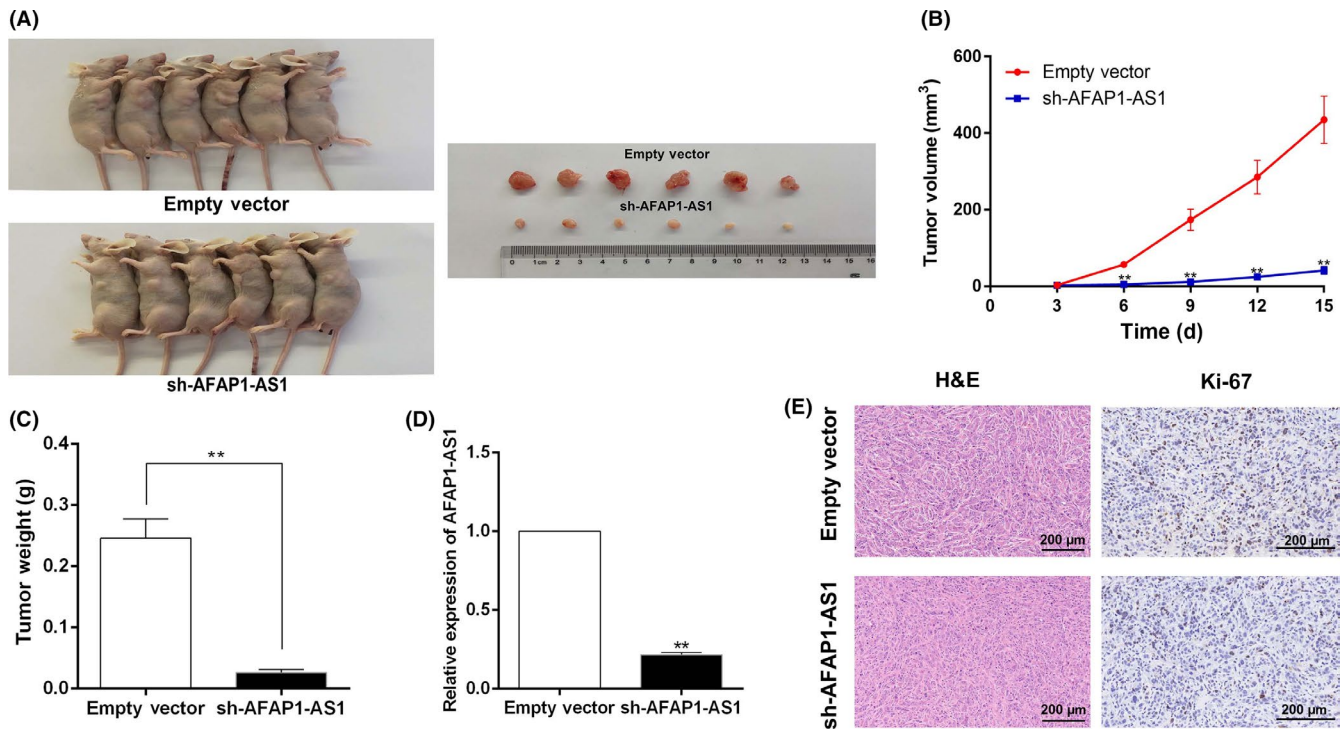


**FIGURE 4** Effect of actin filament-associated protein 1 antisense RNA 1 (AFAP1-AS1) knockdown on tumor growth in vivo. A, B, Nude mouse model of non-small-cell lung cancer induced with PC-9 cell stably transfected with sh-AFAP1-AS1 or empty vector was established to observe the effects of AFAP1-AS1 on the transplanted carcinoma. Tumor volume was measured every 3 d. C, Average weight of transplanted tumors from respective groups. D, AFAP1-AS1 levels were detected in xenograft tumors by quantitative real-time PCR. E, Tumor tissues formed from PC-9/sh-AFAP1-AS1 showed lower Ki-67 protein levels than those formed from PC-9/empty vector. Left, H&E staining; right, immunohistochemical staining

Our previous studies showed that lncRNAs could repress the transcription of downstream genes by interacting with histone modifying enzymes or other RNA-binding proteins.<sup>22-24</sup> As such, we used RIP assays to identify potential interactions between AFAP1-AS1 and other well-known RNA-binding proteins including LSD1, EZH2, and SUZ12 (two subunits of polycomb repressive complex 2 [PRC2]). We found that AFAP1-AS1 directly bound LSD1 and EZH2 in PC-9 and H1975 cells (Figure 5B). Then we identified novel genes and transcripts that altered expression between control and AFAP1-AS1-knockdown PC-9 cells by RNA transcriptome sequencing. Among the 1013 differentially expressed transcripts (fold-change  $\geq 2$ ,  $q$  value  $\leq 0.05$ ), 517 transcripts were upregulated and the remaining 496 transcripts were downregulated (Figure 5C, Table S2). Differentially expressed genes were classified according to GO terms, followed by GO enrichment analysis. Our data identified biological processes that included pathways involved in cell proliferation and cell migration ( $P < .05$ , Figure 5D). We then selected several upregulated genes that act as tumor suppressors in multiple cancers for further validation. Quantitative RT-PCR assays were carried out in both PC-9 and H1975 cells to examine levels of *XAF1*, *DMGDH*, and other related genes after knocking down AFAP1-AS1. The results showed that AFAP1-AS1 knockdown upregulated the expression of *XAF1*, *HBP1*, and other genes in both PC-9 and H1975 cells, but no significant differences were observed in the levels of *DMGDH*, *CPEB3*, or *GBP2* after H1975 cells were transfected with si-AFAP1-AS1. Among these AFAP1-AS1-regulated genes, the well-described

transcriptional repressor HBP1 showed relatively higher fold-change in AFAP1-AS1-depleted H1975 cells (Figure 5E). Western blot assays confirmed that HBP1 protein levels were also upregulated in NSCLC cells following AFAP1-AS1 knockdown (Figure 5F).

We next explored whether AFAP1-AS1 led to decreased HBP1 expression through its interaction with LSD1 or EZH2 in PC-9 and H1975 cells by evaluating HBP1 mRNA levels in NSCLC cells transfected with siRNAs against LSD1 and EZH2. Interestingly, qRT-PCR results showed that downregulation of LSD1 increased HBP1 expression, whereas EZH2 knockdown did not (Figures S1B and 5G). Moreover, western blot analysis showed that silencing LSD1 led to increased HBP1 protein levels in PC-9 and H1975 cells. Furthermore, we detected HBP1 expression following LSD1 knockdown in NCI-H1299 cells, which have the lowest AFAP1-AS1 expression. The results showed no significant change, indicating that LSD1 knockdown-induced HBP1 upregulation is partly dependent on AFAP1-AS1 (Figure 5H). Western blot assays confirmed that AFAP1-AS1 did not influence LSD1 protein levels in PC-9 or H1975 cells (Figure S1C).

To explore whether LSD1 can act by binding to the HBP1 promoter, we synthesized primers across 2000 base pairs of the HBP1 promoter region. Chromatin immunoprecipitation assays confirmed that the protein LSD1 could interact with the DNA sequence of the HBP1 promoter regions, where it mediated demethylation of lysine 4 on histone H3; furthermore, AFAP1-AS1 knockdown reduced this

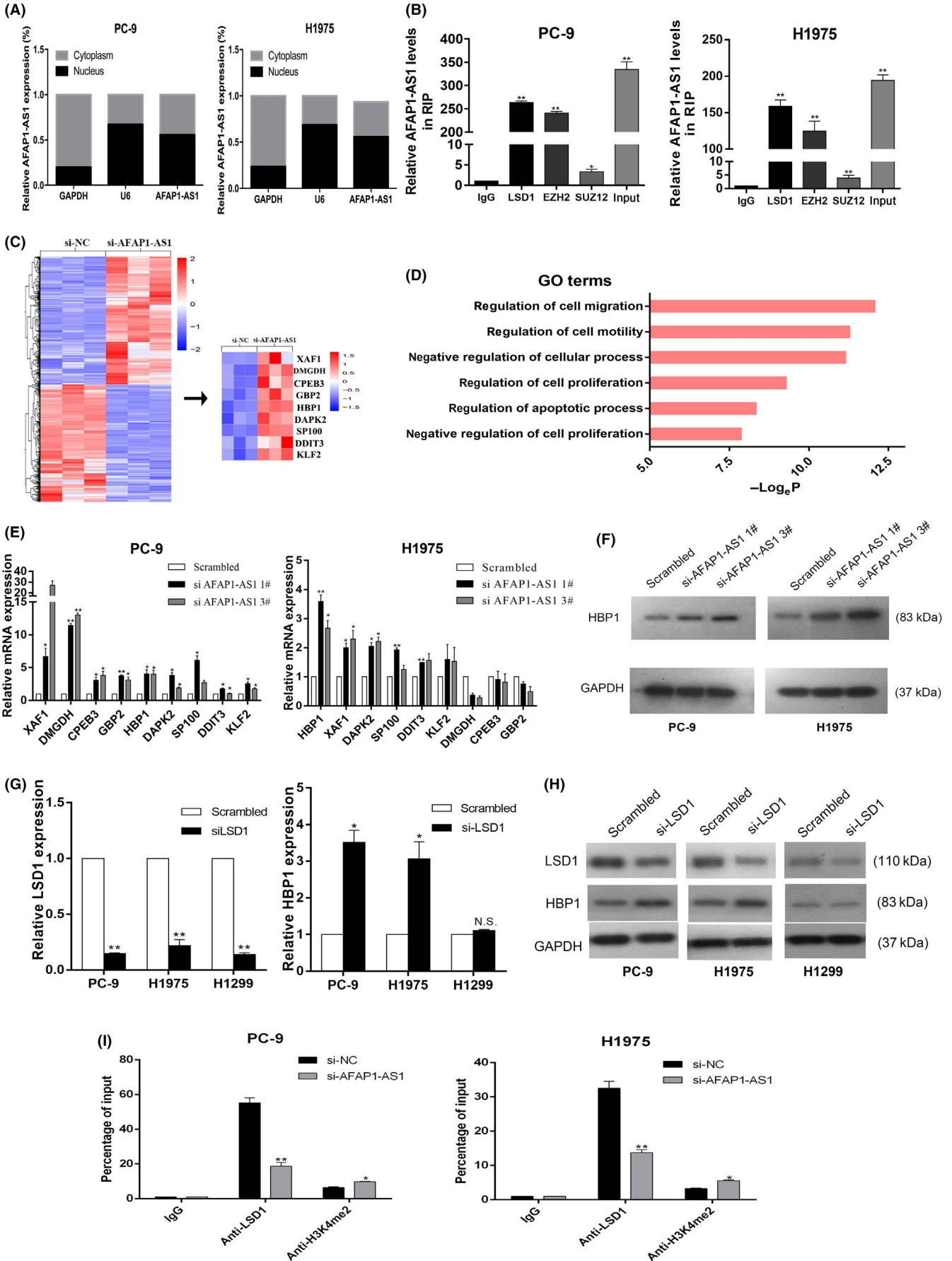


**FIGURE 5** Actin filament-associated protein 1 antisense RNA 1 (AFAP1-AS1) interacts with lysine-specific demethylase 1 (LSD1) to regulate HMG box-containing protein 1 (HBP1) in non-small-cell lung cancer cells. A, Relative expression of AFAP1-AS1 in PC-9 and H1975 cell cytoplasm and nucleus using quantitative real-time (qRT)-PCR. GAPDH was used as a cytoplasm marker and U6 was used as a nuclear marker. B, RNA immunoprecipitation assays were undertaken in PC-9 and H1975 cells, expression levels of AFAP1-AS1 RNA was detected by qRT-PCR and presented based on the fold enrichment in LSD1, EZH2, and SUZ12 immunoprecipitates relative to IgG immunoprecipitates. C, Heatmap of gene alteration in AFAP1-AS1 knockdown PC-9 cells compared to control cells. D, Gene Ontology analysis for all genes with altered expressions between the negative control group and AFAP1-AS1 knockdown group cells in vitro. E, qRT-PCR was used to verify mRNA expression levels of tumor suppressors in scrambled siRNA and si-AFAP1-AS1 1#/3# transfected PC-9 and H1975 cells. F, HBP1 protein levels in AFAP1-AS1 knockdown PC-9 and H1975 cells transfected with si-AFAP1-AS1 1# or si-AFAP1-AS1 3#. G,H, qRT-PCR and western blot assays were used to detect LSD1 and HBP1 mRNA and protein levels in PC-9, H1975, and H1299 cells treated with si-LSD1. I, ChIP-qRT-PCR of LSD1 occupancy and H3K4me2 binding in the HBP1 promoter regions in PC-9 and H1975 cells transfected with si-AFAP1-AS1 or scrambled siRNA

interaction in PC-9 and H1975 cells (Figure 5I). These findings indicated that AFAP1-AS1 mediated epigenetic changes of HBP1, recruiting LSD1 and resulting in HBP1 transcription repression in lung cancer cells.

### 3.6 | Overexpression of HBP1 inhibited NSCLC cell proliferation

To elucidate the biological role of HBP1 in NSCLC cells, we undertook an overexpression functional assay. Quantitative RT-PCR and western blot assays showed that HBP1 expression was increased in PC-9 and H1975 cells transfected with the pcDNA-HBP1 vector (Figure 6A). The CCK-8 and colony formation assays revealed that cell proliferation was impaired following HBP1 overexpression (Figure 6B,C). Additionally, flow cytometry indicated that HBP1 up-regulation mildly induced G<sub>1</sub>/G<sub>0</sub> arrest and apoptosis in PC-9 and H1975 cells (Figure 6D,E). Furthermore, we used qRT-PCR assays to detect AFAP1-AS1 and HBP1 mRNA levels in 20 NSCLC tissues, and the results indicated a negative correlation between the two (Figure 6F), which was also confirmed in the NSCLC patient profile of GEO (GSE19804) (Figure 6G).

Finally, we undertook rescue assays to confirm whether HBP1 was involved in the oncogenic activity of AFAP1-AS1 in NSCLC cells. To this end, PC-9 and H1975 cells were cotransfected with AFAP1-AS1- and HBP1-targeted siRNAs. The CCK-8 and colony formation assays showed that the inhibition of NSCLC cell proliferation was partially rescued after cotransfection with si-AFAP1-AS1 and si-HBP1 compared with NSCLC cells transfected with si-AFAP1-AS1 alone (Figure 7A,B). Western blot analysis showed that si-HBP1 transfection could partly rescue si-AFAP1-AS1-increased HBP1 expression (Figure 7C). Taken together, these findings confirmed that the oncogenic functions of AFAP1-AS1 in NSCLC cells were, at least in part, through repressing HBP1 expression.

## 4 | DISCUSSION

Recently, many studies have reported the connection of lncRNAs with tumorigenesis and cancer progression. For example, lncRNAs including HOTAIR, TUG1, PVT1, and MEG3, have been shown to play crucial roles in NSCLC development by regulating transcriptional or posttranscriptional processes.<sup>[10, 25-28]</sup> For example, lncRNA PVT1

promotes expression of hypoxia-inducible factor-1 $\alpha$  in NSCLC by functioning as a competing endogenous RNA for miR-199a-5p, and is a vital potential target for NSCLC hypoxia therapy.<sup>29</sup> Our previous study showed that lncRNA 00152 was upregulated in lung adenocarcinoma tissues compared with normal samples and promoted lung adenocarcinoma cell proliferation through EZH2-mediated interleukin-24 silencing.<sup>30</sup> In this study, we identified another lncRNA, AFAP1-AS1, that was also upregulated in NSCLC tissues and cells. High AFAP1-AS1 expression could potentially be pursued as a prognostic marker for poor outcomes in NSCLC patients. Additionally, AFAP1-AS1 downregulation slowed NSCLC cell proliferation in vitro and tumor growth in vivo. Although Yin et al<sup>31</sup> reported that AFAP1-AS1 could epigenetically silence p21 transcription in A549 cells, we selected PC-9 and H1975 cells with higher AFAP1-AS1 expression to discover specific downstream target genes influenced by AFAP1-AS1, which requires more research evidence to better explain the biological processes of NSCLC.

To our knowledge, many lncRNAs contribute to malignant cancer cell phenotypes by actively governing the expression of local or distal genes. A general mechanistic picture has emerged in which lncRNAs modulate transcription through the recruitment of chromatin modifiers. Interactions between lncRNAs and histone-modifying complexes are prominent with respect to PRC2, which mediates the methylation of lysine 27 on histone 3, and the lysine-specific demethylase LSD1, which is a flavin-dependent amine oxidase that is highly selective for demethylation of lysine 4 on histone H3 to function as a transcription corepressor, but also functions as a transcription coactivator through the demethylation of lysine 9 on histone H3.<sup>5</sup> One prominent example is lncRNA HOTAIR, which mediates transcriptional gene silencing by binding to the PRC2 and LSD1/CoREST/REST complexes and directing them to the specific gene sites.<sup>32</sup> Additionally, Lv et al reported that LSD1 overexpression promotes proliferation, migration, and invasion in NSCLC, and Kozub et al reported that LSD1 is upregulated in several solid tumors, including neuroblastoma and estrogen receptor-negative breast cancers, where it is associated with poor patient outcomes and aggressive clinicopathological features.<sup>33,34</sup> These data suggested that the association between LSD1 and lncRNAs is clearly important in malignancy.

In the present study, we used RIP assays to reveal that AFAP1-AS1 directly binds to LSD1 in lung cancer cells. RNA transcriptome sequencing of AFAP1-AS1 knockdown PC-9 cells revealed increased

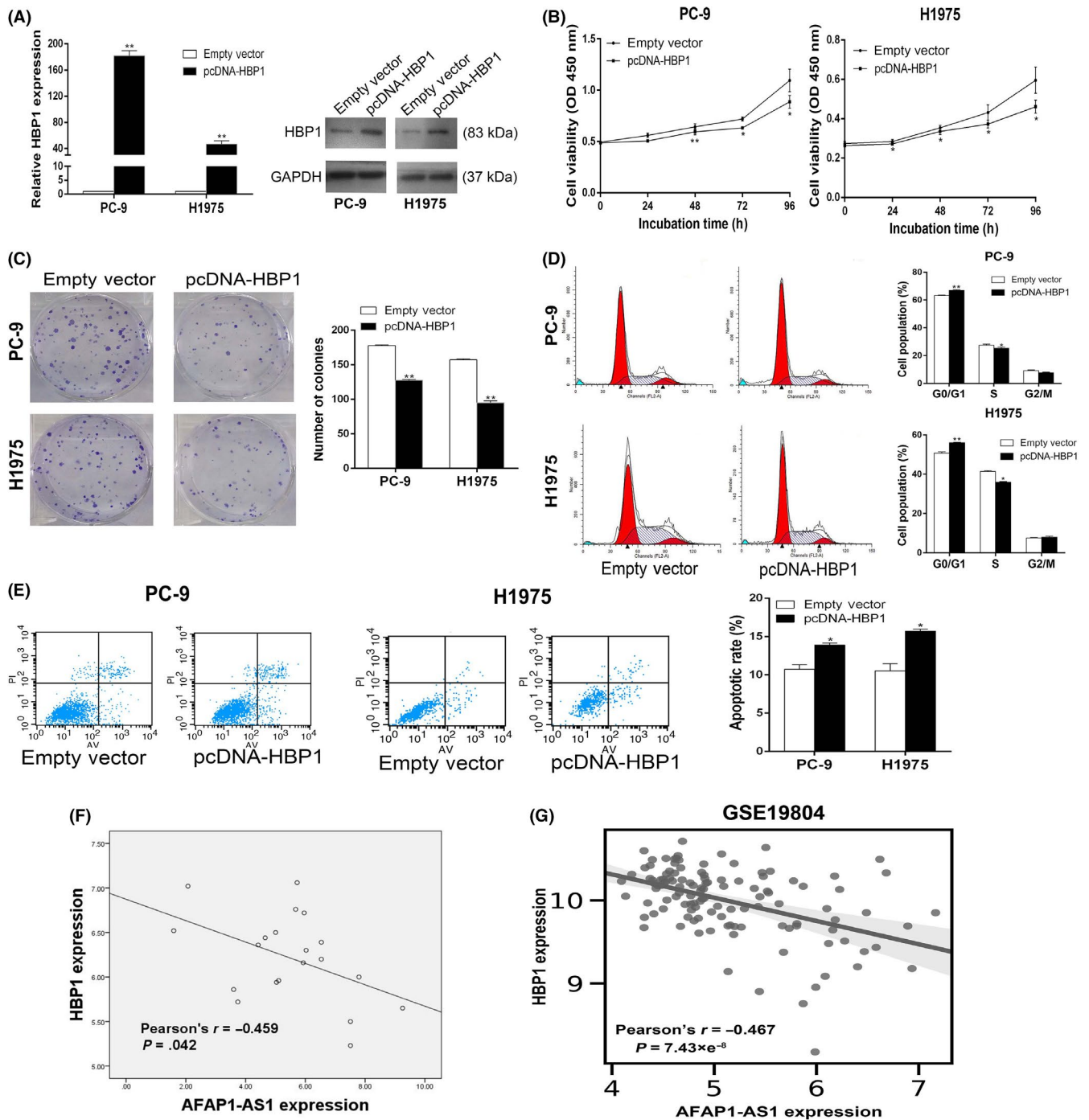


**FIGURE 6** Effects of HMG box-containing protein 1 (HBP1) overexpression on PC-9 and H1975 cells in vitro. A, mRNA and protein levels of HBP1 in PC-9 and H1975 cells transfected with pcDNA-HBP1. B, C, CCK-8 and colony formation analysis were undertaken to detect cell viability. D, E, Flow cytometry were used to determine cell cycle and apoptotic rates of PC-9 and H1975 cells transfected with pcDNA-HBP1 or empty vector. F, Analysis of correlation between actin filament-associated protein 1 antisense RNA 1 (AFAP1-AS1) and HBP1 mRNA levels (Dct value compared with GAPDH) in non-small-cell lung cancer tissues ( $n = 20$ ). G, Relationship between AFAP1-AS1 and HBP1 expression was analyzed in the profile of non-small-cell lung cancer patient tissue from Gene Expression Omnibus

expression of the tumor suppressor HBP1, suggesting it was a novel target of AFAP1-AS1 in NSCLC cells. Interestingly, knocking down LSD1 in PC-9 and H1975 cells increased HBP1 expression, and ChIP assays showed that AFAP1-AS1 could recruit LSD1 to the promoter regions of HBP1 and repress its transcription by mediating the

demethylation of H3K4me2. These data indicated that AFAP1-AS1 plays vital roles in LSD1-mediated HBP1 repression in NSCLC cells.

HMG box-containing protein 1 is a member of the HMG-box transcription factor family and functions as a transcriptional repressor. It has two important domains including the HMG box DNA-binding

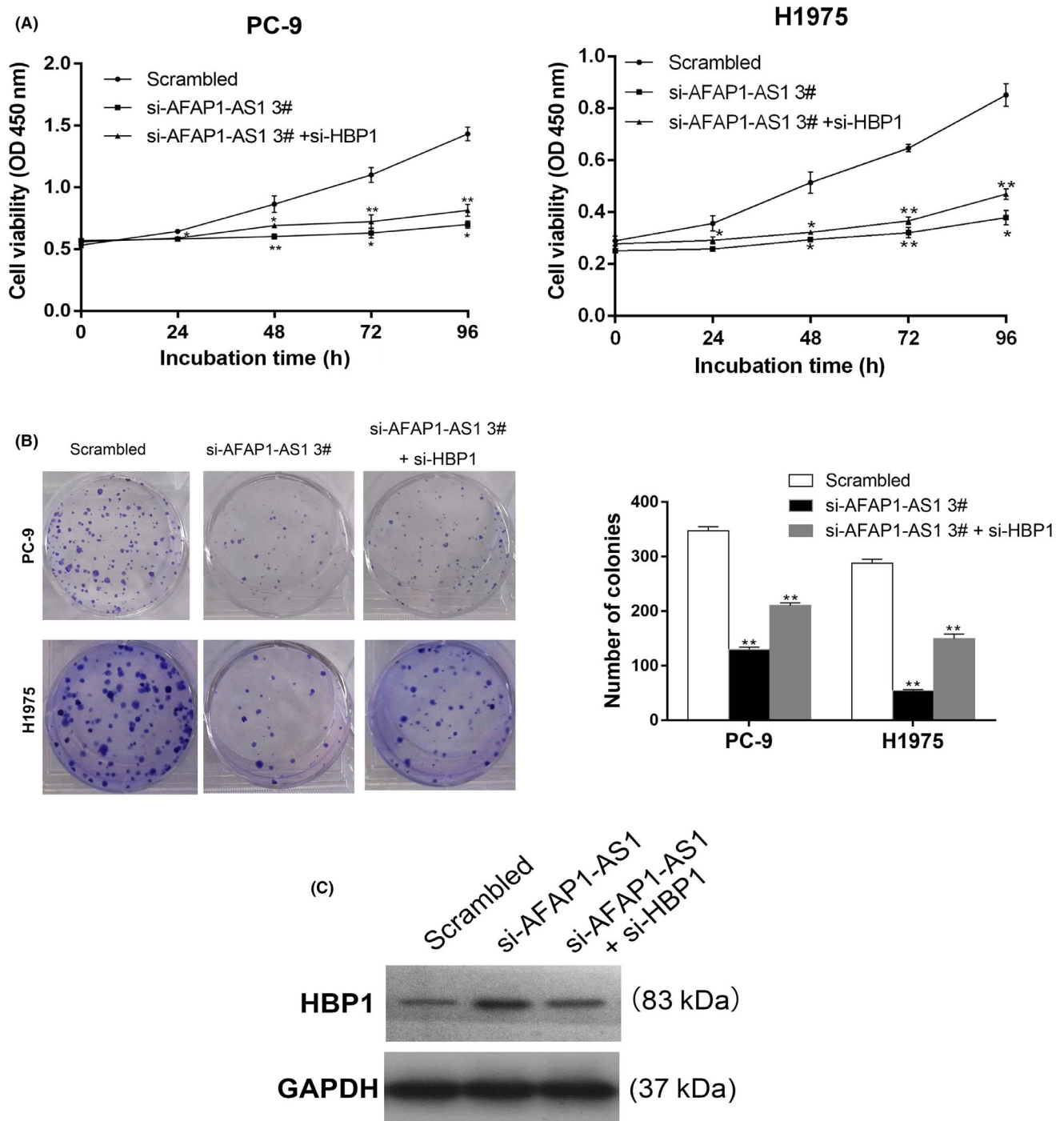


**FIGURE 7** Actin filament-associated protein 1 antisense RNA 1 (AFAP1-AS1) promotes non-small-cell lung cancer cell proliferation partly through negative regulation of HMG box-containing protein 1 (HBP1). A, B, CCK-8 and colony formation assays showed that si-AFAP1-AS1 and si-HBP1 cotransfection could partly reverse cell proliferation abilities of PC-9 and H1975 cells transfected with si-AFAP1-AS1. C, Western blot analysis of the level of HBP1 in PC-9 cells transfected with si-AFAP1-AS plus si-HBP1 or si-AFAP1-AS1 alone

domain and an AXH domain.<sup>35</sup> HMG box-containing protein 1 has been found to have tumor-suppressive functions in multiple cancers. For instance, HBP1 overexpression sensitizes prostate cancer cells to radiation and increases apoptosis in prostate cancer cells.<sup>36</sup> In oral cancer, increased HBP1 expression is associated with decreased cell growth following N-acetylcysteine treatment.<sup>37</sup> In a separate study on breast

cancer, Li and colleagues ascribed the decrease in HBP1 expression to miR-17-5p upregulation, promoting cell proliferation, invasion, and migration.<sup>38</sup> HMG box-containing protein 1 inhibits the progression from G<sub>1</sub> to S phase of the cell cycle by regulating several key genes involved in cell proliferation, such as CDKN2A (p16 INK4A) and CDKN1A (p21 CIP1), and also contributes to oncogenic RAS-induced senescence

and terminal cell differentiation, supporting the hypothesis that HBP1 acts as a tumor suppressor.<sup>39</sup> As HBP1 mRNA/protein expression is reduced in NSCLC patients due to promoter hypermethylation, we found that HBP1 overexpression inhibited lung cancer cell proliferation and cell cycle progression and slightly induced apoptosis.<sup>40</sup> Finally, decreasing HBP1 expression partially reversed the inhibition of proliferation in lung cancer cells following AFAP1-AS1 knockdown. The results indicated that HBP1 acts as a tumor suppressor and its inhibition plays an important role in the malignant phenotype of NSCLC.

In conclusion, our findings showed that AFAP1-AS1 is upregulated in NSCLC tissues and cells, and that high AFAP1-AS1 expression in NSCLC patients suggests worse outcomes. Furthermore, AFAP1-AS1 can promote NSCLC cell proliferation and migration through epigenetic silencing of tumor suppressor HBP1. Our study could provide a new insight into targeting the AFAP1-AS1/LSD1/HBP1 axis as a treatment strategy for NSCLC patients.

## ACKNOWLEDGEMENTS

This work was supported by grants from the National Natural Science Foundation of China (No. 81672307 and 81871871), the Medical Innovation Team Foundation of the Jiangsu Provincial Enhancement Health Project (No. CXTDA2017021), the "333 high class Talented Man Project" (No. BRA2016509), the Nanjing Science and Technology Development Project (No. 2017sc512046), and the Jiangsu Graduate Scientific Research Innovation Program (No. KYCX18\_1494).

## DISCLOSURE

The authors have no conflicts of interest to declare.

## ORCID

Zhaoxia Wang  <https://orcid.org/0000-0002-1893-371X>

## REFERENCES

- Torre LA, Bray F, Siegel RL, et al. Global cancer statistics, 2012. *CA Cancer J Clin*. 2015;65(2):87-108.
- Cho JH. Immunotherapy for non-small-cell lung cancer: current status and future obstacles. *Immune Netw*. 2017;17(6):378-391.
- Rosell R, Karachaliou N. Lung cancer: maintenance therapy and precision medicine in NSCLC. *Nat Rev Clin Oncol*. 2013;10(10):549-550.
- Beermann J, Piccoli MT, Viereck J, et al. Non-coding RNAs in development and disease: background, mechanisms, and therapeutic approaches. *Physiol Rev*. 2016;96(4):1297-1325.
- Akhade VS, Pal D, Kanduri C. Long noncoding RNA: genome organization and mechanism of action. *Adv Exp Med Biol*. 2017;1008:47-74.
- Dhamija S, Diederichs S. From junk to master regulators of invasion: lncRNA functions in migration, EMT and metastasis. *Int J Cancer*. 2016;139(2):269-280.
- Khorkova O, Hsiao J, Wahlestedt C. Basic biology and therapeutic implications of lncRNA. *Adv Drug Deliv Rev*. 2015;87:15-24.
- Yang G, Lu X, Yuan L. LncRNA: a link between RNA and cancer. *Biochim Biophys Acta*. 2014;1839(11):1097-1109.
- Xu TP, Liu XX, Xia R, et al. SP1-induced upregulation of the long noncoding RNA TINCR regulates cell proliferation and apoptosis by affecting KLF2 mRNA stability in gastric cancer. *Oncogene*. 2015;34(45):5648-5661.
- Liu J, Wan L, Lu K, et al. The long noncoding RNA MEG3 contributes to cisplatin resistance of human lung adenocarcinoma. *PLoS ONE*. 2010;10(5):e0114586.
- Chen X, Chen Z, Yu S, et al. Long noncoding RNA LINC01234 functions as a competing endogenous RNA to regulate CBFB expression by sponging miR-204-5p in gastric cancer. *Clin Cancer Res*. 2018;24(8):2002-2014.
- Wu W, Bhagat TD, Yang X, et al. Hypomethylation of noncoding DNA regions and overexpression of the long noncoding RNA, AFAP1-AS1, in Barrett's esophagus and esophageal adenocarcinoma. *Gastroenterology*. 2013;144(5):956-966.e4.
- Zhuang Y, Jiang H, Li H, et al. Down-regulation of long non-coding RNA AFAP1-AS1 inhibits tumor cell growth and invasion in lung adenocarcinoma. *Am J Transl Res*. 2017;9(6):2997-3005.
- Ye Y, Chen J, Zhou Y, et al. High expression of AFAP1-AS1 is associated with poor survival and short-term recurrence in pancreatic ductal adenocarcinoma. *J Transl Med*. 2015;13:137.
- Feng Y, Zhang Q, Wang J, et al. Increased lncRNA AFAP1-AS1 expression predicts poor prognosis and promotes malignant phenotypes in gastric cancer. *Eur Rev Med Pharmacol Sci*. 2017;21(17):3842-3849.
- Shi X, Zhang H, Wang M, et al. LncRNA AFAP1-AS1 promotes growth and metastasis of cholangiocarcinoma cells. *Oncotarget*. 2017;8(35):58394-58404.
- Han X, Wang L, Ning Y, et al. Long non-coding RNA AFAP1-AS1 facilitates tumor growth and promotes metastasis in colorectal cancer. *Biol Res*. 2016;49(1):36.
- He B, Zeng J, Chao W, et al. Serum long non-coding RNAs MALAT1, AFAP1-AS1 and AL359062 as diagnostic and prognostic biomarkers for nasopharyngeal carcinoma. *Oncotarget*. 2017;8(25):41166-41177.
- Bo H, Gong Z, Zhang W, et al. Upregulated long non-coding RNA AFAP1-AS1 expression is associated with progression and poor prognosis of nasopharyngeal carcinoma. *Oncotarget*. 2015;6(24):20404-20418.
- Guo JQ, Li SJ, Guo GX. Long noncoding RNA AFAP1-AS1 promotes cell proliferation and apoptosis of gastric cancer cells via PTEN/p-AKT pathway. *Dig Dis Sci*. 2017;62(8):2004-2010.
- Zhang JY, Weng MZ, Song FB, et al. Long noncoding RNA AFAP1-AS1 indicates a poor prognosis of hepatocellular carcinoma and promotes cell proliferation and invasion via upregulation of the RhoA/Rac2 signaling. *Int J Oncol*. 2016;48(4):1590-1598.
- Sun M, Nie F, Wang Y, et al. LncRNA HOXA11-AS promotes proliferation and invasion of gastric cancer by scaffolding the chromatin modification factors PRC2, LSD1, and DNMT1. *Cancer Res*. 2016;76(21):6299-6310.
- Huang M, Hou J, Wang Y, et al. Long noncoding RNA LINC00673 is activated by SP1 and exerts oncogenic properties by interacting with LSD1 and EZH2 in gastric cancer. *Mol Ther*. 2017;25(4):1014-1026.
- Nie F, Yu X, Huang M, et al. Long noncoding RNA ZFAS1 promotes gastric cancer cells proliferation by epigenetically repressing KLF2 and NKD2 expression. *Oncotarget*. 2017;8(24):38227-38238.
- Wu JL, Meng FM, Li HJ. High expression of lncRNA MEG3 participates in non-small cell lung cancer by regulating microRNA-7-5p. *Eur Rev Med Pharmacol Sci*. 2018;22(18):5938-45.
- Guo D, Wang Y, Ren K, et al. Knockdown of lncRNA PVT1 inhibits tumorigenesis in non-small-cell lung cancer by regulating miR-497 expression. *Exp Cell Res*. 2018;362(1):172-179.

27. Jiang C, Yang Y, Yang Y, et al. Long noncoding RNA (lncRNA) HOTAIR affects tumorigenesis and metastasis of non-small cell lung cancer by upregulating miR-613. *Oncol Res*. 2018;26(5):725-734.
28. Lin PC, Huang HD, Chang CC, et al. Long noncoding RNA TUG1 is downregulated in non-small cell lung cancer and can regulate CELF1 on binding to PRC2. *BMC Cancer*. 2016;16:583.
29. Wang C, Han C, Zhang Y, et al. LncRNA PVT1 regulate expression of HIF1alpha via functioning as ceRNA for miR-199a-5p in non-small cell lung cancer under hypoxia. *Mol Med Rep*. 2018;17(1):1105-1110.
30. Chen QN, Chen X, Chen ZY, et al. Long intergenic non-coding RNA 00152 promotes lung adenocarcinoma proliferation via interacting with EZH2 and repressing IL24 expression. *Mol Cancer*. 2017;16(1):17.
31. Yin D, Lu X, Su J, et al. Long noncoding RNA AFAP1-AS1 predicts a poor prognosis and regulates non-small cell lung cancer cell proliferation by epigenetically repressing p21 expression. *Mol Cancer*. 2018;17(1):92.
32. Cai B, Song XQ, Cai JP, et al. HOTAIR: a cancer-related long non-coding RNA. *Neoplasma*. 2014;61(4):379-391.
33. Lv T, Yuan D, Miao X, et al. Over-expression of LSD1 promotes proliferation, migration and invasion in non-small cell lung cancer. *PLoS ONE*. 2012;7(4):e35065.
34. Kozub MM, Carr RM, Lomber GL, et al. LSD1, a double-edged sword, confers dynamic chromatin regulation but commonly promotes aberrant cell growth. *F1000Research*. 2017;6:2016.
35. Lee MF, Hsieh NT, Huang CY, et al. All trans-retinoic acid mediates MED28/HMG box-containing protein 1 (HBP1)/beta-catenin signaling in human colorectal cancer cells. *J Cell Physiol*. 2016;231(8):1796-1803.
36. Chen Y, Wang Y, Yu Y, et al. Transcription factor HBP1 enhances radiosensitivity by inducing apoptosis in prostate cancer cell lines. *Anal Cell Pathol (Amst)*. 2016;2016:7015659.
37. Lee MF, Chan CY, Hung HC, et al. N-acetylcysteine (NAC) inhibits cell growth by mediating the EGFR/Akt/HMG box-containing protein 1 (HBP1) signaling pathway in invasive oral cancer. *Oral Oncol*. 2013;49(2):129-135.
38. Li H, Bian C, Liao L, et al. miR-17-5p promotes human breast cancer cell migration and invasion through suppression of HBP1. *Breast Cancer Res Treat*. 2011;126(3):565-575.
39. Bollaert E, de Rocca Serra A, Demoulin JB. The HMG box transcription factor HBP1: a cell cycle inhibitor at the crossroads of cancer signaling pathways. *Cell Mol Life Sci*. 2019;76(8):1529-1539.
40. Tseng RC, Huang WR, Lin SF, et al. HBP1 promoter methylation augments the oncogenic beta-catenin to correlate with prognosis in NSCLC. *J Cell Mol Med*. 2014;18(9):1752-1761.

## SUPPORTING INFORMATION

Additional supporting information may be found online in the Supporting Information section at the end of the article.

**How to cite this article:** Yu S, Yang D, Ye Y, et al. Long noncoding RNA actin filament-associated protein 1 antisense RNA 1 promotes malignant phenotype through binding with lysine-specific demethylase 1 and repressing HMG box-containing protein 1 in non-small-cell lung cancer. *Cancer Sci*. 2019;110:2211-2225. <https://doi.org/10.1111/cas.14039>